Gilbert Reibnegger*

An *ab initio* and density functional theory study on neutral pterin radicals

DOI 10.1515/pterid-2015-0008 Received May 8, 2015; accepted June 29, 2015; previously published online August 7, 2015

Abstract: The electronic structures of the five radicals resulting from homolytic elimination of one of the hydrogen atoms from the most stable tautomeric form of neutral pterin were investigated in gas phase as well as in aqueous solution. Molecular wave functions obtained by density functional theory were analysed by quantum theory of atoms in molecules and electron localisation functions (ELF). Spin densities of the radicals as well as electrostatic potential functions were analysed. Radicals resulting from elimination of N-bonded hydrogen atoms are more stable in comparison with radicals obtained after abstraction of C-bonded hydrogen atoms. N-centred radicals show strong delocalisation of spin density over both heteroaromatic rings; in C-centred radicals delocalisation does not occur. ELF analyses showed that in N-derived radicals particularly the lone electron pair at N,' is strongly involved into the bicyclic heteroaromatic π -electron system. Thereby, bonding geometry at N₂' in these radicals changes from pyramidal to planar. Transition from gas phase to solution phase (water) generally leads to increased polarity of the structures. Pterin-derived free radicals have been implicated in several biologically important reactions; so this investigation provides first insights into the detailed electronic structures of such molecular systems.

Keywords: density functional theory; electron localisation function; electronic structure; pterin radicals; quantum theory of atoms in molecules; spin density.

Introduction

The heteroaromatic compound pteridine (pyrazine-[2,3-d]-pyrimidine) contains four ring nitrogen atoms which are

*Corresponding author: Gilbert Reibnegger, Institute of Physiological Chemistry, Center of Physiological Medicine, Medical University of Graz, A-8010 Graz, Austria, E-mail: gilbert.reibnegger@medunigraz.at responsible for a remarkably complex chemical behaviour of pteridine itself and also of the many derivatives thereof. A large variety of pteridine derivatives occur in apparently all living organisms, exerting a multitude of different biochemical/biological functions that are only partially understood. In several investigations, pteridine radicals have been detected experimentally, or at least pteridine derivatives were observed to modulate the reactivity of other free radicals [1–18].

Recently, several studies were published reporting on the results of quantum chemical calculations of the detailed electronic structures of pterin (2-amino-3H-pteridine-4-on) and derivatives employing density functional theory (DFT) with reasonably sized basis sets [19-22]. In the present investigation, I report on such calculations extended to the five radicals derived from the most stable tautomeric form of neutral pterin by homolytic elimination of each one of the five hydrogen atoms present in pterin. In order to get a sound understanding of the effects of radical formation on the pterin molecule, detailed analyses of the resulting wave functions using quantum theory of atoms in molecules (QT-AIM) [23] and the electron localisation functions (ELF) [24], as well as evaluations of spin densities and electrostatic potential functions (ESP), are provided. All analyses were performed in gas phase and in polar solution phase (solvent water).

Materials and methods

Computational strategy and computer software

Reasonable starting geometries of the five radicals were derived from the minimum energy structure of the most stable tautomer of pterin as obtained in my previous paper [21] simply by successively removing each one of the five hydrogen atoms. These structures were then employed as input geometries for a geometry optimisation at the UBecke3LYP/6-31G(d) level of theory, using the GAUSS-IAN suite of quantum chemistry programs (Gaussian G09W, version 9.5, Gaussian Inc., Pittsburgh, PA, USA). In order to ensure that the geometries found are indeed minimum energy structures, frequency calculations were performed at the same level of theory. As for all structures exclusively positive vibrational frequencies were obtained, all results shown in this paper refer to true minimum energy geometries.

The subsequent computations of final electronic energies, molecular wave functions, electron density distributions and ESP functions for each radical were done using G09W software at the UBecke3LYP/6-311+G(2d,p) level of theory: as shown in [25], the chosen level of theory yields quite accurate results while at the same time being computationally feasible also for medium-sized molecules. Notably, all quantum chemical computations were performed in the gas phase as well as in aqueous solution phase: here, the solvation model based on density (SMD) method [26] was employed. The SMD model is a continuum solvation model based on quantum mechanical charge density of a solute molecule interacting with a continuum description of the solvent. Full electron density is employed without defining partial atomic charges. The model is universally applicable to charged or uncharged solute molecules in any solvent for which a few key descriptors such as the dielectric constant, the refractive index, the bulk surface tension and the acidity and basicity parameters are known.

A possible problem in unrestricted quantum chemical calculation is spin contamination, i.e. the artificial mixing of different electronic spin states. DFT results generally appear to be less sensitive to this problem than Hartree-Fock models [27]. In order to judge if spin contamination might have an effect on the reported results, the deviation of the average expectation value <S $^2>$ from its eigenvalue S(S+1)=0.75 (for pure doublet states with S=1/2) was recorded for all radical structures.

In-depth QT-AIM analysis (computation of the critical points of the electron density functions as well as the molecular graphs and the gradient paths) and visualisation of QT-AIM results (atomic partial charges and numerical estimates of spin densities integrated over the atomic basins of attraction as well as bond delocalisation indices) were done using the program AIMStudio Version 13.11.04 Professional (TK Gristmill Software, Todd A. Keith, Overland Park, KS, USA).

The delocalisation index is obtained from the Fermi hole density. It is a measure of the number of electrons that are shared or exchanged between two atoms or basins of attraction, and it is directly related to the bond order; a study [28] has shown a linear relationship between both measures for CC, NN, GeGe, C-Si, C-Ge and CN bonds.

The ELF calculations were performed with program DGrid, version 4.6, friendlily provided by Dr. Miroslav Kohout and Dr. Alexey

Baranov, both from Max Planck Institute for Chemical Physics of Solids, Noethnitzer Str. 40, 01187 Dresden, Germany.

Finally, visualisations of the electron density functions, the spin density functions and the ESP of the molecules were done using AVS Express 5.3 software (Advanced Visual Systems Inc., Waltham, MA, USA). Graphs showing the ELF were produced by the open source program Paraview, version 4.01, 32 bit, obtained from www.paraview.org.

Results and discussion

Figure 1 shows the chemical formulae of pterin and the five radicals derived thereof. For pterin, also the conventional numbering system of the second-row atoms is given. Further, the two hydrogens at N₂' are labelled "a" and "b" in order to distinguish the two possible radicals derived by their homolytic elimination. The five radicals derived from pterin by homolytic elimination of a hydrogen atom are, consequently, labelled "N(3)", "N(2') $_{a}$ ", "N(2') $_{b}$ ", "C(6)" and "C(7)". The geometries of all radicals were optimised using Ubecke3LYP/6-31G(d) level of theory; by frequency analyses, all optimised geometries were shown to be true minimum states. The final electronic energies of the five radicals, obtained with the extended basis set 6-311+G(2d,p) using the optimised geometries, are listed in Table 1 for the gas phase as well as for the aqueous solution phase. The table in addition gives the comparison of these energies (plus the energy of a free hydrogen atom) with that of the most stable tautomer of neutral pterin, computed at the same level of theory [21]. Interestingly, the relative ordering of the radicals according to their stabilities is slightly different in gas phase as compared to solution phase: in the gas phase, the most stable radical is radical N(2'), followed by N(3) (+4.8 kcal/mol) and N(2'),

Figure 1: Chemical formulae of pterin and the five radicals derived thereof by homolytically removing, one by one, each of the five hydrogen atoms. In the formula of pterin, the conventional numbering system of the atoms is included.

Table 1: Electronic energies of the five radicals and their comparison (together with that of a free hydrogen atom) with the electronic energy of the most stable tautomer of neutral pterin (final computation at the UBecke3LYP/6-311+G(2d,p) level of theory).

Molecule	Electronic energy (Hartree)	Electronic energy plus free H ^b [Hartree] in gas and solution phase	E(radical)+E(H)–E(pterin), kcal/mol ^c	E(radical)–E(radical) _{min} , kcal/mol
Pterina		_		
Gas phase	-580.828463			
Solution	-580.868687			
N(3)				
Gas phase	-580.157270	-580.659426	106.1	4.8
Solution	-580.197669	-580.697661	107.3	0.0
N(2') _a				
Gas phase	-580.164843	-580.666999	101.3	0.0
Solution	-580.196589	-580.696581	108.0	0.7
N(2') _b				
Gas phase	-580.155224	-580.657380	107.4	6.0
Solution	-580.195453	-580.695445	108.7	1.4
C(6)				
Gas phase	-580.147365	-580.649521	112.3	11.0
Solution	-580.182395	-580.682387	116.9	9.6
C(7)				
Gas phase	-580.150921	-580.653077	110.1	8.7
Solution	-580.186323	-580.686315	114.4	7.1

Energy of neutral pterin at same level of theory is taken from reference [21]. Energy of free hydrogen atom at same level of theory:

(+6.0 kcal/mol). The C-centred radicals C(7) (+8.7 kcal/mol) and C(6) (+11.0 kcal/mol) are more unstable than the N-centred structures. In water, however, the most stable radical is N(3), slightly more stable than N(2'), (+0.7 kcal/mol) and $N(2')_{h}$ (+1.4 kcal/mol). The energy gaps to the C-centred radicals are, again, quite substantial: C(7) (+7.1 kcal/mol) and C(6) (+9.6 kcal/mol).

Table 1 also permits a comparison of the electronic energies of the five radicals in gas phase versus solution phase: N(3), -24.0 kcal/mol; N(2')₂, -18. 6 kcal/mol; N(2')_b, -23.9 kcal/mol; C(6), -20.6 kcal/mol and C(7), -20.9 kcal/mol. Thus, stabilisation of the molecules by solvation with water is largest for N(3) and smallest for N(2'), which explains the changed stability order in gas versus solution phase.

Importantly, while neutral pterin as well as the C-centred radicals C(6) and C(7) exhibit non-planar geometries at the N₂'-atom, the three N-centred radicals show strictly planar structures. For neutral pterin, the pyramidal bonding geometry at the N₂ atom was already described earlier [21]. To describe the pyramidal bonding geometry, the torsional angles N_3 - C_2 - N_2 '- H_a (α) and N_1 - C_2 - $N_2'-H_b(\beta)$ are used: in the gas phase, neutral neopterin has α =-32.6° and β =11.6° (note that both hydrogens are situated on the same side of the plane of the pterin ring; the different signs of the torsional angles are just due to their specification). In solution phase, α reduces to -16.9°, and

 β rises to 13.6°. For radical C(6), we find in the gas phase α =-32.6° and β =11.5°, while in aqueous solution phase α =-17.0° and β =13.4°. Similarly, in C(7) in the gas phase α =-29.6° and β =11.5°; in solution phase, α =-10.2° and β =8.6°. In contrast, in the three N-centred radicals these torsional angles are invariably smaller than 1°.

Spin contamination, a possible problem in such calculations, was quite small in all cases; the expectation value <S²> did not deviate markedly from its ideal value of 0.75 for a pure doublet state: radical N(3), 0.7856 (gas) and 0.7778 (aqueous solution phase); radical N(2'), 0.7899 (gas) and 0.7893 (aqueous solution phase); radical N(2'), 0.7910 (gas) and 0.7895 (aqueous solution phase); radical N(6), 0.7559 (gas) and 0.7561 (aqueous solution phase); and radical N(7), 0.7555 (gas) and 0.7555 (aqueous solution phase).

Figure 2 shows, for pterin as well as the five radicals derived thereof, the molecular graphs together with the atomic partial charges obtained by applying QT-AIM to the wave functions of the energy-minimised geometries of the molecules in the gas phase (black numbers) and in the aqueous solution phase (red numbers, if different from the gas phase). (Ring critical points as well as ring paths were intentionally not drawn in order to improve clarity.) With few exceptions, most partial charges are larger in solution phase. Thus, the aqueous solution leads to increased polarity of neutral pterin as well as of the radicals. The

^{-0.502156} Hartree (gas phase); -0.499992 Hartree (solution). 'Conversion factor: 1 a.u.=627.5095 kcal/mol.

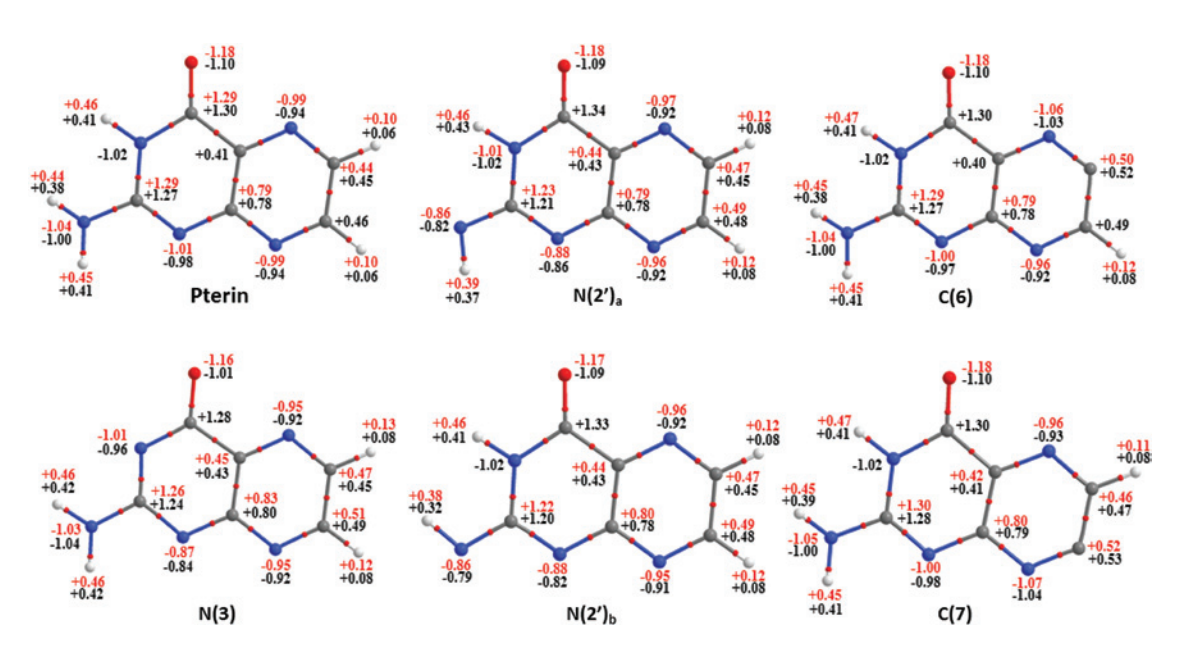


Figure 2: The molecular graphs of optimised geometries of pterin and the five radicals and their atomic partial charges resulting from QT-AIM analyses.

The radicals are denoted by the position of the hydrogen atoms missing with respect to neutral pterin. Atoms are represented by the atomic critical points (large dots, coloured as usual: dark grey, carbon; light grey, hydrogen; red, oxygen; blue, nitrogen). The small red dots between two bonded atoms represent the bond critical bonds. The bond paths (connecting atomic critical points and bond critical bonds) are coloured according to the bonded atoms. Ring critical points and ring paths are not shown for clarity. Numbers in black denote the atomic partial charges in the gas phase; those in red show the charges in solution phase (water) if different from those in the gas phase.

strongest increase in (negative) partial charge is seen for the oxygen atom in N(3); this is in accordance with the fact that this radical experiences the largest solvation energy and becomes the most stable radical in solution.

The partial charges of most atoms, shown in Figure 2, do not change greatly when passing from neutral pterin to one of the radicals. However, as Figure 3 demonstrates, effects of radical formation on the ESP functions in every case are observable: the regions with negative ESP become spatially more extended. This is not surprising because hydrogen atoms bonded to nitrogen atoms (and, to a lesser extent, to carbon atoms) carry a positive partial charge. Removal of a hydrogen as neutral atom necessarily results in a redistribution of the electrons in the remaining radicals. The effects are stronger in the case of the N-centred radicals than in their C-centred counterparts, because the positive partial charges of hydrogens bonded to C atoms are considerably smaller than those bonded to N atoms. As Figure 3 additionally demonstrates, the transition from gas to aqueous solution phase also generally increases negative ESP regions, which is in line with the notion of stronger polarity in the solution phase.

In order to better understand the effects of radical formation on the bonding characteristics, Figure 4 reports the delocalisation indices of all bond critical points, indicating the respective bond strengths. Again, results obtained

in the gas phase are denoted with black numbers, and results in solution phase (if different) are marked in red. Generally, the effects of radical formation on the delocalisation indices in the N-centred radicals in relationship to neutral pterin are much more pronounced and observable over larger distances than in the C-centred ones, indicating weaker mesomeric delocalisation in the latter:

In the N(3) radical, the bond strengths of the C_2 - N_3 bond, the N_3 - C_4 bond and the N_1 - C_{8a} bond are markedly increased in comparison with neutral pterin. Even the rather distant C_7 - N_8 bond shows still some strengthening. In contrast, the strength of the N_1 - C_2 bond is much weaker; the strengths of the C_{8a} - N_8 and the C_{4a} - C_{8a} bonds as well as of the C_4 - C_{4a} and the C_6 - C_7 bonds are somewhat lowered.

The strongest increase in bond strengths in the N(2')_a radical is seen for the C₂-N₂' bond; followed by the N₁-C_{8a} and the N₃-C₄ bonds; notable weakening (<0.05 change in delocalisation indices) occurs only for the N₁-C₂ bond.

In the $N(2')_b$ radical, too, the C_2 - N_2' bond is markedly strengthened, and a weaker strengthening is seen for the N_1 - C_{8a} bond. The N_1 - C_2 bond is again much weaker, and some decrease in bond strength is noted for the C_{8a} - N_8 bond.

In the C(6) radical, the strength of the N_5 - C_6 bond is markedly increased, whereas the strength of the adjacent C_{4a} - N_5 bond is decreased; analogously, in the C(7) radical, the strengthening effect is large for the C_7 - N_8 bond, and a

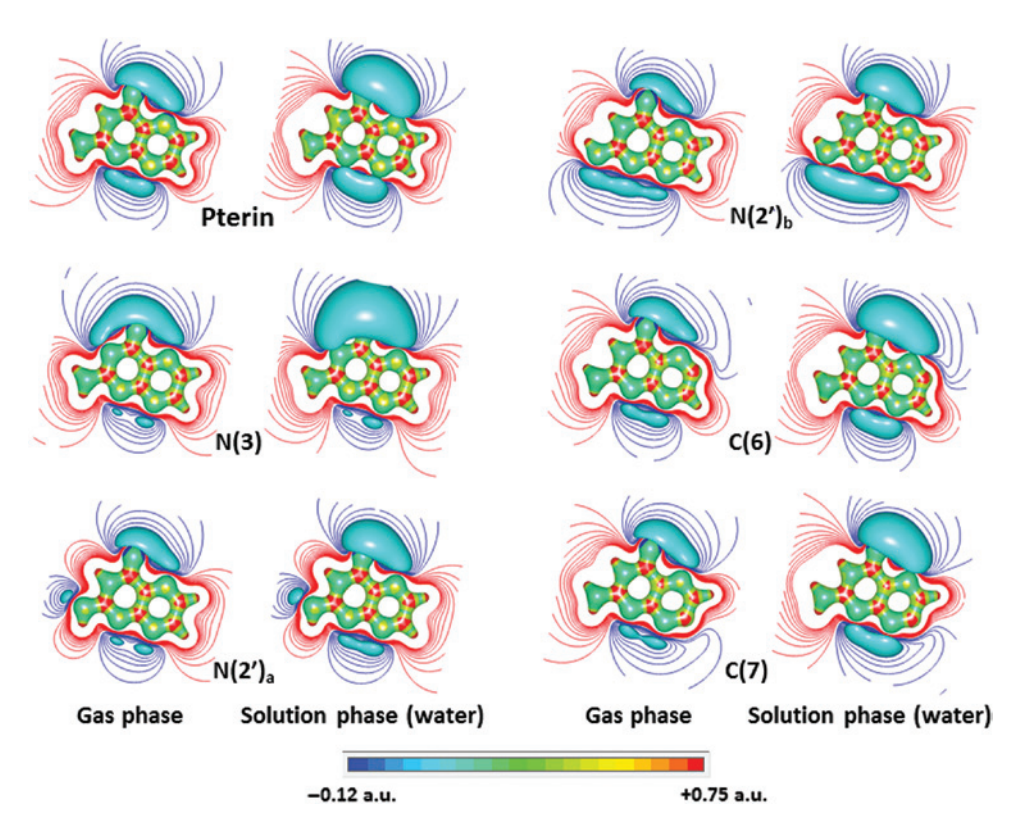


Figure 3: Visualisations of the electron density functions and the ESP of pterin and the five radicals in the gas phase as well as in solution phase (water).

The molecules are represented by the isodensity surfaces at 0.10 a.u. of electron density function, coloured according to the local ESP (for the colour code, see bottom of the Figure). Blue ESP contours: negative ESP from -0.01 a.u. (outermost contour) in steps decreasing at -0.01 a.u. steps. Red ESP contours: positive ESP from +0.01 a.u. (outermost contour) increasing at +0.01 a.u. steps. For these plots, electron density functions and ESP functions are evaluated by program G09W at regular 192×192×192 cubes surrounding the molecular structures.

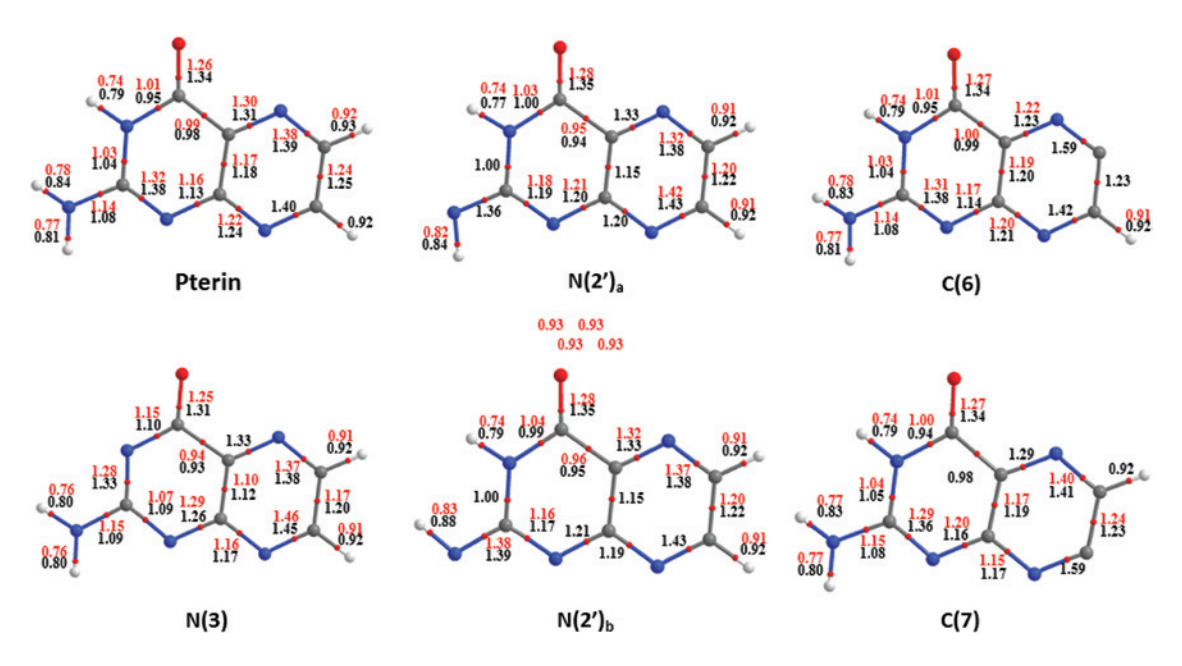


Figure 4: The molecular graphs of optimised geometries of pterin and the five radicals and the bond delocalisation indices resulting from QT-AIM analyses. Numbers in black denote the delocalisation indices in the gas phase; those in red show the respective values in solution phase (water) if different from those in the gas phase.

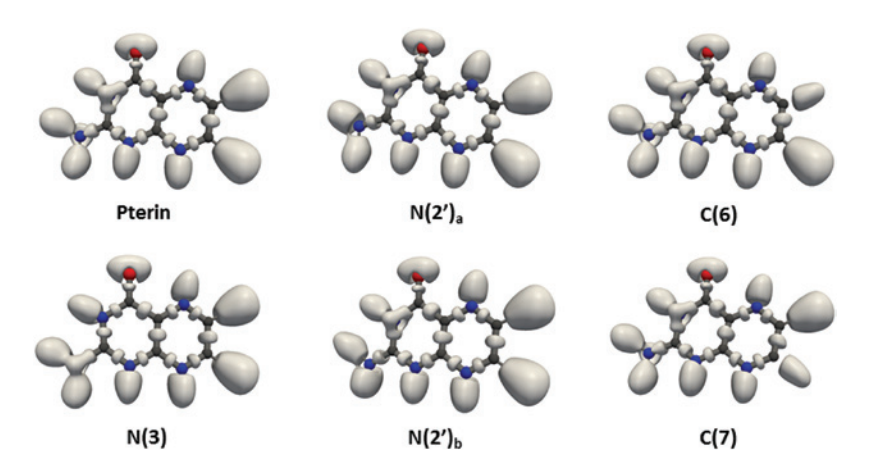


Figure 5: Electron localisation functions (ELF) of pterin and the five radicals in the gas phase. The ELF isosurfaces are plotted at a value of 0.80 a.u.

decrease is observed for the strength of the adjacent $\rm C_{8a}$ - $\rm N_8$ bond. Thus, the formation of both C-centred radicals has practically no effect on the delocalisation indices in the pyrimidine moiety.

As a graphical representation of the effects of radical formation on the bonding details, Figure 5 shows ELF isosurfaces of pterin and the five radicals in the gas phase (in solution phase, the figures are essentially unchanged). In the N(3) radical we note that the lone electron pair at N₃, being involved in a marked amide resonance with the adjacent C=O bond in pterin and in all four other radicals, now is much stronger located at the N₃ atom and no longer takes part in the bond system of the pyrimidine moiety. Thus, the observed strengthening effect on the C₂-N₃ bond is mainly due to the partial formation of a new double bond

involving the unpaired electron of N_3 and one electron of the original N_1 and C_2 double bond, formally leaving an unpaired electron on N_1 . The lone pair at N_3 is not involved in this new double bond. Moreover (and in accordance with the notion of the differences between non-planar and planar bond structures at N_2 in the course of geometry optimisation), in the N(3) as well as in the $N(2')_a$ and $N(2')_b$ radicals, the ELF structure at N_2 is symmetrical with respect to the molecular plane (planar geometry), while in pterin and in the two C-centred radicals C(6) and C(7) the ELF structure at N_2 appears like a distorted tetrahedron in line with the non-planar geometry.

Figure 6 shows the spin density functions of the radicals, represented by isosurfaces at spin densities +0.05 a.u. (blue) and -0.05 a.u. (red). A solution effect was seen only

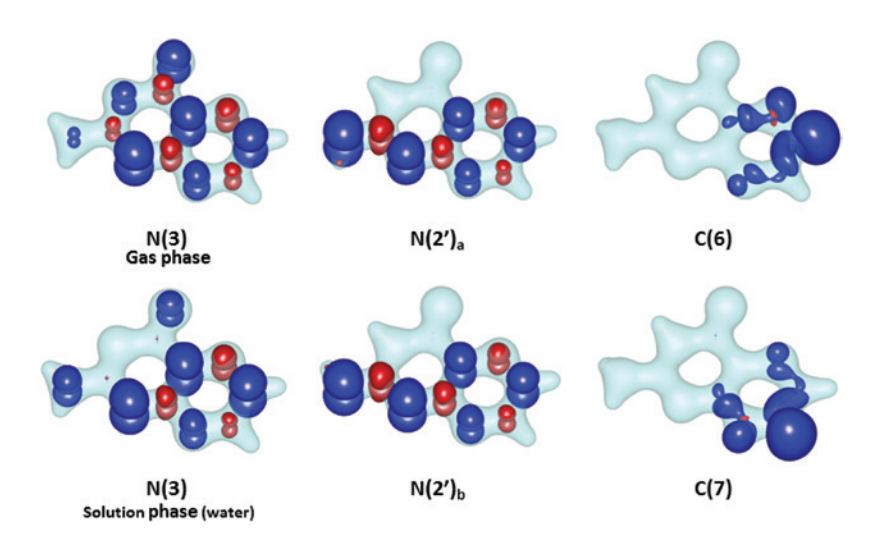


Figure 6: Spin densities of the pterin radicals, grouped according to N-centred versus C-centred radicals.

The visualisations show the spin density functions embedded in an isodensity surface of the electron density function at 0.15 a.u (light grey). The spin density function isosurfaces are shown at +0.05 a.u. (blue) and -0.05 a.u. (red). As differences between the gas phase and the aqueous solution phase are only visible for radical N(3), the results are shown in both phases only for this structure.

for radical N(3); the pictures showing the spin densities of the other four radicals in solution phase are virtually indistinguishable from those in the gas phase and are therefore not shown. The striking differences between the three N-centred and the two C-centred radicals become evident. Obviously, in the N-centred radicals there exists a remarkably strong delocalisation of the unpaired electron; in fact, not only the pyrimidine moieties where radical formation actually takes place but also the pyrazine parts show notable spin densities. As an extreme example for the delocalisation, note that in the N(3) radical in the gas phase, only a small portion of the positive spin density (0.07) is located at N₂ itself; about 0.40 is found at N₃; and the remaining positive spin density is observed at C., C₆, N₈ and O. This is even more so in aqueous solution, where the spin density at N₃ completely vanishes and spin density at the N_2 atom is increased. In the $N(2')_a$ and $N(2')_b$ radicals, about 0.45 of the positive spin density stays with N₂, and the remaining positive spin density is distributed between N₁, C₆, C₆ and N₈. Interestingly, in these two radicals, no spin density is observed in the amide portion of the pyrimidine moiety. This may indicate that in these structures, the strong amide resonance between the N atom and the (formal) C=O group prevents the (formally possible) inclusion of the O atom in the delocalisation of the unpaired electron due to the predominantly singlebond character of the carbon-oxygen bond. This feature clearly distinguishes the N(3) radical from the latter two radicals. In all cases, the spin density isosurfaces show the typical symmetry characteristics of π -electrons, indicating that the delocalisation of the unpaired electron occurs exclusively via the π -electron system. In contrast, delocalisation of the unpaired electron is very weak in the C-centred radicals; the overwhelming portion of the positive spin density (more than 0.70) remains located at the site of radical formation, and the remaining positive spin density is restricted to the immediate vicinity of the affected atoms. The pyrimidine parts remain completely unaffected from formation of the C-centred radicals. In comparison with the N-centred radicals, we note in addition that the symmetry of the spin density isosurfaces is markedly different from that observed in the N-centred radicals; obviously here the effects are influencing, if at all, only the neighbouring σ -bonds. (The negative spin densities [red isosurfaces] are - in absolute numbers - in all cases smaller than 0.10).

Figure 7 finally provides a possible scheme of mesomeric structures for radical N(3) which may explain the spin density distribution of this radical as seen in Figure 6. Similar schemes could be drawn for radicals N(2'), and $N(2)_{b}$. Interestingly, a non-vanishing spin density on N_{2}

Figure 7: A scheme of possible resonance structures for radical

seems to require some transfer of electronic charge from this atom to the oxygen atom (via the vinylogous amide structure), and this resonance structure appears to be somewhat stabilised by aqueous solution, while at the same time the spin density on the oxygen atom is reduced. In addition it might be noted that in radicals N(2'), and N(2), while an analogous resonance structure with spin density on the oxygen atom is formally equally possible as in radical N(3), such a structure obviously is not realised – in these radicals no spin density is present on the oxygen atom. For radicals C(6) and C(7), resonance structures involving the π -electron system cannot be drawn; consequently, the spin density can be "delocalised", if at all, only via the σ-electron system to the nearest neighbours of the affected C-atoms.

Conclusion

To the best of my knowledge, this is the first investigation on detailed electronic structures of radicals derived from pterin. In this paper, I have restricted attention to the five radicals resulting from homolytic elimination of hydrogen atoms from neutral pterin. Even in this limited selection of possible radicals, important features of such systems became evident, and distinct effects of solution in polar environment in comparison with the gas phase were found. An extension of this study towards the large variety of other pteridine systems in different oxidation states as well as in various ionic states would certainly be of considerable interest to enlarge the theoretical basis for understanding the complex chemistry and biochemistry of these substances under various conditions in terms of their electronic properties.

The investigation has revealed fundamental differences between the N-centred and the C-centred radicals of pterin: while in the former mesomeric delocalisation of the unpaired electron causes rather strong effects of radical formation essentially over the whole molecule, in the latter such delocalisation does not occur, and the effects of radical formation remain locally restricted. Solution in polar media like water generally increases polarities of the structures and causes noticeable shift in charge distributions and, partly, in distribution of spin densities. Particularly the analyses of quantum-chemically computed wave-functions by various techniques like QT-AIM and ELF estimation provide rich and detailed insight into the electronic and structural properties of such radicals.

Finally, this work provides further evidence that problems with spin contamination appear to have only minute effects in DFT modelling of pterin-derived radicals.

References

- Oettl K, Dikalov S, Freisleben H-J, Mlekusch W, Reibnegger G. Spin trapping study of antioxidant properties of neopterin and 7,8-dihydroneopterin. Biochem Biophys Res Commun 1997:234:774–8.
- Watanabe K, Arai T, Mori H, Nakao S, Suzuki T, Tajima K, et al. Pterin-6-aldehyde, an inhibitor of xanthine oxidase, has superoxide anion radical scavenging activity. Biochem Biophys Res Commun 1997;233:447–50.
- 3. Wede I, Altindag ZZ, Widner B, Wachter H, Fuchs D. Inhibition of xanthine oxidase by pterins. Free Rad Res 1998;29:331–8.
- Hurshman AR, Krebs C, Edmondson DE, Huynh BH, Marletta MA. Formation of a pterin radical in the reaction of the heme domain of inducible nitric oxide synthase with oxygen. Biochemistry 1999;38:15689–96.
- Oettl K, Reibnegger G. Pteridines as inhibitors of xanthine oxidase: structural requirements. Biochem Biophys Acta 1999:1430:387–95.
- Oettl K, Wirleitner B, Baier-Bitterlich G, Grammer T, Fuchs D, Reibnegger G. Formation of oxygen radicals in solutions of 7,8-dihydrobiopterin. Biochem Biophys Res Commun 1999;264:262–7.
- 7. Oettl K, Greilberger J, Reibnegger G. Dihydroneopterin as a scavenger of nitrogen centered radicals. Pteridines 2000;11:90–3.
- Oettl K, Pfleiderer W, Reibnegger G. Formation of oxygen radicals in solutions of different 7,8-dihydropterins: quantitative structure-activity relationships. Helv Chim Acta 2000; 83:954–65.
- Schmidt PP, Lange R, Gorren AC, Werner ER, Mayer B, Anderson KK.
 Formation of a protonated trihydrobiopterin radical cation in the first reaction cycle of neuronal and endothelial nitric oxide

- synthase detected by electron paramagnetic resonance spectroscopy. J Biol Inorg Chem 2001;6:151–8.
- Wirleitner B, Czaputa R, Oettl K, Böck G, Widner B, Reibnegger G, et al. Induction of apoptosis by 7,8-dihydroneopterin: involvement of radical formation. Immunobiol 2001;203: 629-41.
- Oettl K, Reibnegger G. Pteridine derivatives as modulators of oxidative stress. Curr Drug Metabol 2002;3:203-9.
- 12. Wei C-C, Wang Z-Q, Hemann C, Hilles R, Stuehr DJ. A tetrahydrobiopterin radical forms and then becomes reduced during N∞-hydroxyarginine oxidation by nitric oxide synthase. J Biol Chem 2003;278:46668−73.
- 13. Oettl K, Greilberger J, Reibnegger G. Modulation of free radical formation by pterine derivatives. Pteridines 2004;15:97–101.
- 14. Wei C-C, Wang Z-Q, Tejero J, Yang Y-P, Hemann C, Hille R, et al. Catalytic reduction of a tetrahydrobiopterin radical within nitric oxide synthase. J Biol Chem 2008;283:11734–42.
- Martinéz A, Barbosa A. Are pterins able to modulate oxidative stress? Theor Chem Acc 2010;127:485–92.
- Woodward JJ, NetatyJahromy Y, Britt RD, Marletta MA. Pterincentered radical as a mechanistic probe of the second step of nitric oxide synthase. J Am Chem Soc 2010;132:5105–13.
- 17. Oliveros E, Dántola ML, Vignoni M, Thomas AH, Lorente C. Production and quenching of reactive oxygen species by pterin derivatives, an intriguing class of biomolecules. Pure Appl Chem 2011;83:801–11.
- 18. Ji H-F, Shen L. Mechanistic study of ROS-photogeneration by pterin. Pteridines 2011;22:73-6.
- 19. Soniat M, Martin CB. Theoretical study on the relative energies of neutral pterin tautomers. Pteridines 2008;19:120-4.
- 20. Soniat M, Martin CB. Theoretical study on the relative energies of anionic pterin tautomers. Pteridines 2009;20:124–9.
- 21. Reibnegger G. QT-AIM analysis of neutral pterin and its anionic and cationic forms. Pteridines 2014;25:41–8.
- 22. Nekkanti S, Martin CB. Theoretical study on the relative energies of cationic pterin tautomers. Pteridines 2015;26:13-22.
- 23. Bader RW. Atoms in molecules: a quantum theory. Oxford University Press: Oxford, UK, 1990.
- Becke AD, Edgecombe KE. A simple measure of electron localization in atomic and molecular systems. J Chem Phys 1990;92:5397–403.
- Foresman JB, Frisch AE. Exploring chemistry with electronic structure methods, 2nd ed. Gaussian Inc.: Pittsburgh, PA, USA, 1996.
- Marenich AV, Cramer CJ, Truhlar DG. Universal solvation model based on solute electron density and on a continuum model of the solvent defined by the bulk dielectric constant and atomic surface tensions. J Phys Chem B 2009;113:6378–96.
- Montoya A, Truong TN, Sarofim, AF. Spin contamination in Hartree-Fock and density functional theory wavefunctions in modelling of adsorptions on graphite. J Phys Chem A 2000;104:6108–10.
- 28. Firme CL, Antunes OA, Esteves PM. Relation between bond order and delocalization index of QTAIM. Chem Phys Lett 2009;468:129-33.